AIP Conference Proceedings

Triple-junction solar cell performance under Fresnel-based concentrators taking into account chromatic aberration and off-axis operation

P. Espinet-González, R. Mohedano, I. García, P. Zamora, I. Rey-Stolle et al.

Citation: AIP Conf. Proc. **1477**, 81 (2012); doi: 10.1063/1.4753839

View online: http://dx.doi.org/10.1063/1.4753839

View Table of Contents: http://proceedings.aip.org/dbt/dbt.jsp?KEY=APCPCS&Volume=1477&Issue=1

Published by the American Institute of Physics.

Triple-junction Solar Cell Performance Under Fresnel-based Concentrators Taking Into Account Chromatic Aberration And Off-axis Operation

P. Espinet-González[1], R. Mohedano[2], I. García[1], P. Zamora[1], I. Rey-Stolle[1], P. Benitez[1,2], C. Algora[1], A. Cvetkovic[2], M. Hernández[2], J. Chaves[2], J.C. Miñano[1,2], Y. Li[1]

[1] Universidad Politécnica de Madrid (UPM), Madrid, (Spain), [2] LPI, Altadena, CA, USA

Abstract. Concentration photovoltaic (CPV*)* systems might produce quite uneven irradiance distributions (both on their level and on their spectral distribution) on the solar cell. This effect can be even more evident when the CPV system is slightly off-axis, since they are often designed to assure good uniformity only at normal incidence. The non-uniformities both in absolute irradiance and spectral content produced by the CPV systems, can originate electrical losses in multi-junction solar cells (MJSC). This works is focused on the integration of ray-tracing methods for simulating the irradiance and spectrum maps produced by different optic systems throughout the solar cell surface, with a 3D fully distributed circuit model which simulates the electrical behavior of a state-of-the-art triple-junction solar cell under the different light distributions obtained with ray-tracing. In this study four different CPV system (SILO, XTP, RTP, and FK) comprising Fresnel lenses concentrating sunlight onto the same solar cell are modeled when working on-axis and 0.6 degrees off-axis. In this study the impact of non-uniformities on a CPV system behavior is revealed. The FK outperforms other Fresnel-based CPV systems in both on-axis and off-axis conditions.

Keywords: Fresnel lens, nonimaging, solar concentrator, Köhler integration, CPV, multi-junction solar cells
PACS: 42.15.Eq, 42.79.Ek, 88.40.F, 88.40.H, 88.40.jj, 88.40.fc, 88.40.jp, 81.05.Ea

INTRODUCTION

The nature of MJSC is such that their performance is in most cases based on an optimal usage of a given sun spectrum to achieve a balanced photocurrent generation among the junctions that are series-connected. However, the optics of every CPV system introduces its own spectral effects, not only due to the characteristics of the materials used in each case, but to their optical architecture itself.

The main goal of this work is to combine two enhanced modeling tools (ray-tracing and 3D distributed models) to compare the performance of four different types of Fresnel-based concentrator systems on-axis and off-axis, comprising MJSC. The irradiance of each subcell provided by the studied concentrators is obtained by ray-tracing simulations and it is the input parameter for the calculation of the actual power delivered by the cell. The IV curves of the MJSC inside different concentrators are obtained by using an advanced 3D distributed model [1] for triple-junction solar cells with a whole description of the tunnel junction emulating a commercial-kind triple junction cell.

This work will point out the actual importance of the effect of non-uniformities (irradiance and spectrum) and whether it penalizes some architecture over others.

CPV SYSTEMS ANALYZED

Four Fresnel-based concentrator set-ups have been analyzed in this study: secondary lens doing Köhler integration with 1-fold (SILO), a truncated inverted pyramid mirror (XTP), a truncated inverted pyramid glass (RTP) and secondary lens doing Köhler integration with 4-fold (FK). These systems have been designed for the occasion, trying to optimize their performance using as merit function achieving a good balance between the optical efficiency, acceptance angle and beam output uniformity [2]. For a fair comparison, these concentrators have been designed having similar features (concentration ratio, optical materials) and their full sun spectrum optical behavior have been analyzed through ray tracing.

Figure 1 and table 1 show the main features of the optic systems analyzed in this work.

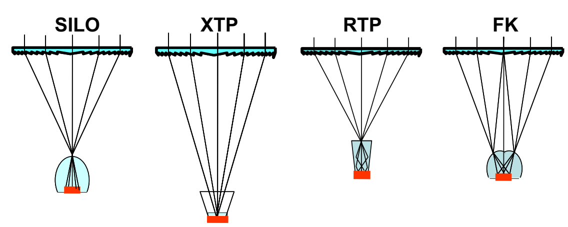

FIGURE 1. Diagonal cross-sections of the CPV systems compared in this work, at scale. The XTP is the deepest one, while the FK and the RTP are the most compact.

8th International Conference on Concentrating Photovoltaic Systems
AIP Conf. Proc. 1477, 81-84 (2012); doi: 10.1063/1.4753839

TABLE 1. Main features of the optics systems analyzed in this work.

Features	SILO	XTP	RTP	FK
C_g	850 X			
POE-cell	270 mm	320 mm	250 mm	250 mm
α	0.85°	0.59°	0.96°	1.14°
f#	1.2	1.4	1.1	1.1
Materials	PMMA for the Fresnel lens, B270 for the glass SOE, ALANOD MIROSILVER for mirror, silicone for the encapsulation, no AR coating on POE or SOE			

CELL AND OPTICS MODELS

One of the keys here is feeding the solar cell distributed model with a map of current densities to assign the corresponding value to the current generators placed all over its area for each junction, in order to simulate the photo-generation at each subcell. This map is deduced from the spectral irradiance patterns produced by each concentrator in the different aiming situations analyzed.

Optical Model

The optical performance of all the concentrators is modeled through ray tracing. The models consider all the spectral features of the different materials and elements involved, and the transmission through the optical trains is analyzed throughout the entire sun spectrum, which fixes the amount of power available within every wavelength range. The values of the refractive index $n(\lambda)$, the absorption coefficient $\alpha_{abs}(\lambda)$ and the reflectivity are all computed in the analysis carried out here, and assigned to the correspondent material.

With the approach followed, not only the local irradiance at each elementary unit of the 3D distributed model is known, but its spectral nature as well. Therefore, the irradiance at each junction throughout the solar cell surface can be obtained using the external quantum efficiency (*EQE*) of each subcell.

Solar Cell Model

The philosophy of the 3D distributed model used in this work to model the electrical behavior of the triple-junction solar cell has been explained in detail elsewhere [1]. This approach consists of dividing the solar cell into elementary units and assigning a suitable circuit model to each unit, depending on its geometry and position in the solar cell area (external contact, metalized, illuminated, or perimeter). The complete solar cell can subsequently be modeled by an electrical circuit that is obtained by interconnecting every unit-circuit with its neighbors. The resulting equivalent circuit formed by thousands of elements is resolved by using a SPICE circuit simulator software package. The elementary units which describe the various solar cell regions are depicted in figure 2. The validation of this model for different illumination conditions including different spatial and spectral inhomogeneities, was presented in [3].

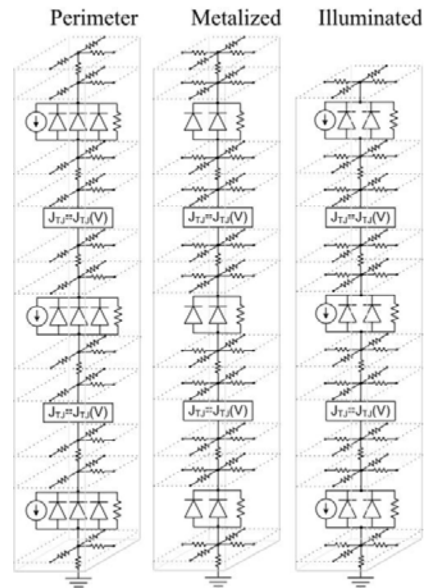

FIGURE 2. Elementary units used for modeling the different regions of a triple-junction solar cell.

The solar cell simulated has an active area of 5.5 mm x 5.5 mm and a front metal grid featuring a comb-like configuration that is comprised of 31 evenly spaced fingers that are 5 µm wide. The busbar is 250 µm wide. The top and middle subcells are current matched at a short circuit current density of 13 mA/cm^2 at 1 sun (900 W/m^2). The bottom cell has a short circuit current density of 20 mA/cm^2 at 1 sun. The bare solar cell used has an efficiency of 40 % for a uniform light profile of 722 X (1 sun = 900 W/m^2).

RESULTS

The performance of the optics + solar cell receivers has been analyzed when they are perfectly aimed at the sun (normal incidence) and when they are somewhat misaligned (0.6 degrees off axis incidence).

At Normal Incidence

Figure 4 (left) shows the irradiance patterns available on the surface of the solar cell for the different optic systems, and split into three ranges of wavelengths fitting with the *EQEs* of the three junctions.

Notice that the FK exhibits the best irradiance uniformity and such uniformity is kept throughout the entire range of sensitive wavelengths. The SILO and RTP achieve decent irradiance uniformity but slightly unbalanced between the TC, MC and BC wavelengths. Finally, the XTP design is less efficient in producing uniformity, showing irradiance peaks 4 times above the average concentration, but the design shown here tries to keep certain balance between the spots produced by different ranges of wavelengths.

The performance of the solar cell under these beams has been calculated. The results are summarized in the IV curves (figure 3) and in table 2.

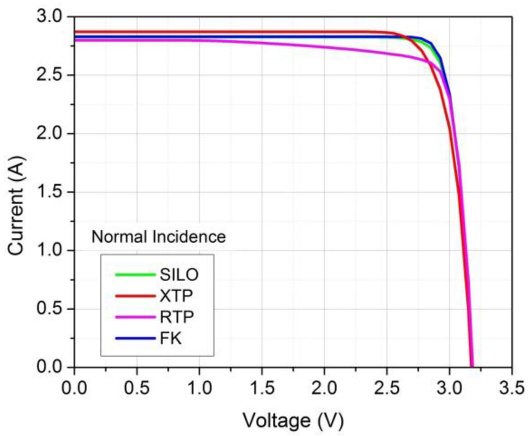

FIGURE 3. MJSC I-V curve at normal incidence

The XTP presents the highest short-circuit current due to the lower absorption losses in the secondary mirror. However, its FF is the lowest one due to the high non-uniform profiles produced which increase the series resistance effects. The RTP also presents a moderate FF. In fact, the photo-generated current begins to decrease at a low voltage (around 1 V). This is because, due to the light profile produced by this optic system, the voltage distribution at each junction of the solar cell makes that at 1 V the recombination diodes in a significant region of one of the subcells are already draining some of the photo-generated current. It has to be noted that the RTP is widely used and this detrimental effect has not been reported. Slight differences in our optical design and in the conditions simulated could have high repercussions on the results. Also, the parameters used in the 3D distributed model (lateral resistances, recombination diodes, etc.) may be slightly pessimistic. Finally, both, the FK and the SILO show a good behavior under normal incidence, presenting the FK the highest efficiency.

TABLE 2. Performance at normal incidence

	SILO	XTP	RTP	FK
Eff(%)	33.69	32.59	32.10	34.17
FF(%)	86.70	82.53	83.41	87.82

At 0.6 Degrees Off-axis

Figure 4 (right) shows the irradiance patterns available on top of the solar cells for the different CPV systems at 0.6° off axis, and again corresponding to each junction in the solar cell.

Notice that the FK still keeps outstanding irradiance uniformity independently of the spectral range of the light. The other systems show important irradiance non uniformities.

In table 3 the optical efficiency ratios between working on-axis and off-axis are shown as well as the ratios of the short circuit current densities under both working conditions. Therefore, if the ratio of the short circuit current densities is lower than the ratio of the optical efficiencies like in the cases of the SILO and the RTP, it reveals that in the off-axis case one of the subcells is draining photo-generated current through the recombination diodes at V = 0V.

TABLE 3. Losses between on-axis and off-axis working conditions.

	SILO	XTP	RTP	FK
$\eta_{opt0.6deg}/\eta_{opt0deg}$	0.95	0.89	0.97	0.99
$J_{sc0.6deg}/J_{sc0deg}$	0.94	0.89	0.87	0.99

The performance of the solar cell under these beams has been calculated. The results are summarized in the *IV* curves presented in figure 5 and in table 4.

The XTP works fairly well under off-axis conditions. The system loses an 11% of the light which is the highest loss among the designs studied because the acceptance angle of this CPV system is the lowest one. The sort circuit current decreases also an 11% due to the light loss. However, the FF does not change significantly revealing that the distribution of the light in off-axis conditions does not have severe repercussions.

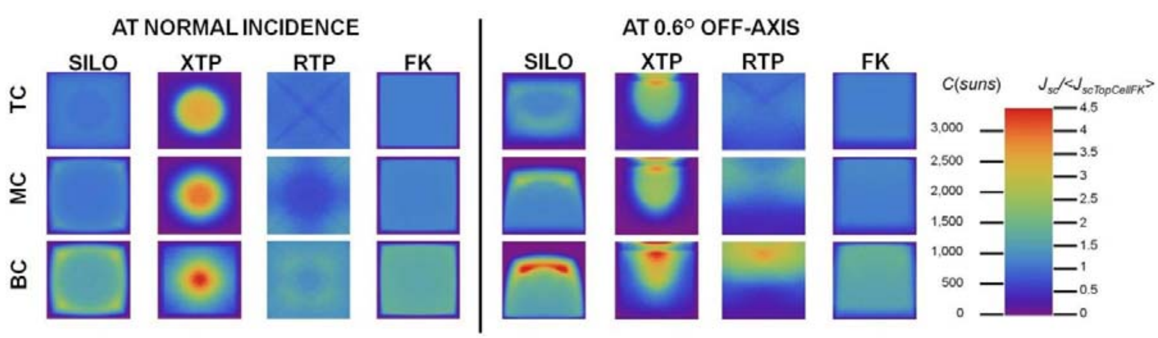

FIGURE 4. Irradiance maps/Normalized photocurrent densities at normal incidence (left) and at 0.6° off-axis incidence (right), for the top cell (TC), middle cell (MC) and bottom cell (BC). 1 sun = 900W/m^2.

The RTP under off-axis conditions noticeably worsens. Even though only a 3% of the light is lost, the short circuit current is 13 % lower than under normal incidence and the current decreases throughout the whole *IV* curve. Therefore, at short circuit current one of the subcells is already draining photo-generated current. The SILO and the FK behaviors on-axis were very similar. However, under off-axis conditions the SILO is considerably worse than the FK. It not only loses more light but also the recombination diodes start draining current at short circuit current. Then, the FK outperforms other Fresnel-based CPV systems in both on-axis and off-axis conditions.

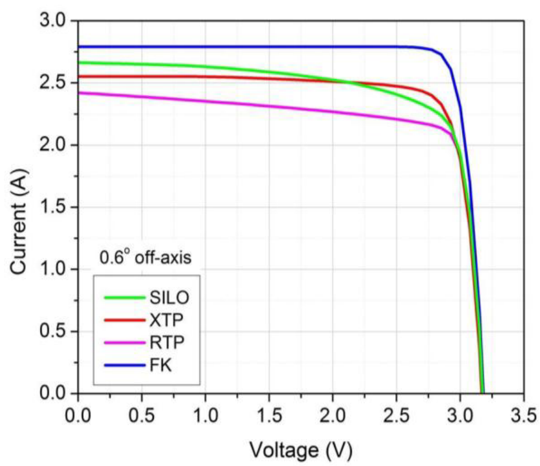

FIGURE 5. MJSC I-V curve at 0.6 deg off-axis incidence

TABLE 4. Performance at 0.6° off-axis

	SILO	**XTP**	**RTP**	**FK**
Eff(%)	27.6	28.8	26.4	33.6
FF(%)	75.4	82.4	79.4	87.6

CONCLUSIONS

In this work ray-tracing simulation for the optics together with 3D distributed models for the MJSC, have been integrated. It has been shown that simulations of the optic systems under the different working conditions expected are essential in order to optimize the whole system design since non uniform irradiance, color separation and low acceptance angles produce substantial performance drops, especially when all effects are combined together. The FK outperforms other Fresnel-based optic systems in both on-axis and off-axis conditions.

ACKNOWLEDGMENTS

The Spanish Ministerio de Ciencia e Innovación has contributed with the INNPACTO program by means of the SIGMAMODULOS IPT-2011-1441-920000 project, project reference TEC2011-28639-C02-01 as well as the Comunidad de Madrid under the NUMANCIA II program (S2009/ENE1477).Support for this work partly comes from the EC and Spanish Ministry MITYC under projects SSL4EU (Grant agreement n º257550, FP7/2007-2013) and V-SS, SMS-IMAGING, V-FL and SMS-AUTO (TSI-020100-2011-445, 372, 381 and 444, Plan Avanza 2011), respectively.

REFERENCES

1. P. Espinet, et. al. "Extended description of tunnel junctions for distributed modelling of concentrator multi-junction solar cells" Solar Energy Materials and Solar Cells, 2011, vol. 95 n9, pp. 2693-2697
2. P. Benítez et. al. "High performance Fresnel-based photovoltaic concentrator", Optics Express, Vol. 18, Issue S1, pp.A25-A40, april 2010
3. I. García et. al. "Extended triple-junction solar cell 3D distributed model: application to chromatic aberration related losses", Proceedings of the 7th International Conference on Concentrating Photovoltaic Systems, April 2011, Las Vegas, Nevada, (USA)